Journal of Sound and Vibration (2001) **247**(3), 527–536
doi:10.1006/jsvi.2001.3639, available online at http://www.idealibrary.com on IDEAL®

LETTERS TO THE EDITOR

COMMENTS ON "THE STABILITY ANALYSIS OF PANTOGRAPH-CATENARY SYSTEM DYNAMICS"

Y. H. Guan and T. C. Lim

Department of Mechanical Engineering, 290 Hardaway Hall, Box 870276, University of Alabama, Tuscaloosa, AL 35487, U.S.A. E-mail: tlim@coe.eng.ua.edu

(*Received* 3 *January* 2001)

1. INTRODUCTION

The authors of references [1, 2] successfully formulated a single-degree-of-freedom linear dynamic model with time-varying stiffness coefficient expressed as

$$\frac{d^2y}{d\tau^2} + 2\zeta\frac{dy}{d\tau} + (1 + \alpha\cos r\tau)y = f, \tag{1}$$

to analyze the dynamics of the pantograph–catenary system typically used in high-speed electric trains. Here, τ is a non-dimensional time (equal to the nominal natural frequency times real time), y is the vertical motion of the pantograph component, f is the uplift forcing term, ζ is the damping ratio, α is the stiffness variation coefficient, and $r > 0$ is a non-dimensional frequency that is proportional to the train speed. Even though the proposed dynamic model given above is relatively simple, the formulation does seem to contain all the critical elements of the problem. However, the presented stability analysis, based on the Floquet theory, appears to be slightly deficient, and does not provide the complete picture of the stable and unstable regions of interest. In this communication, we present the true nature of the actual stability boundaries including the missing transition curves separating stability from instability in the parameter plane (α, r) by applying Hill's method of infinite determinants [3, 4]. Selected cases of stable and unstable free-responses based on our parameter plane result are also verified by employing the 4/5th order Runge–Kutta integration algorithm. Furthermore, equation (1) is transformed into the well-studied standard Mathieu form to reveal additional insight into the dynamic characteristics of the pantograph–catenary system.

2. STABILITY ANALYSIS

Since equation (1) is a class of Mathieu equation, the transition curves separating the bounded and unbounded motions in the parameter plane (α, r) are directly related to the periodic response characterized by periods of either $4\pi/r$ or $2\pi/r$. For a solution of the dynamic motions with periodicity of $4\pi/r$, we can assume the Fourier series

$$y(\tau) = \sum_{n=1}^{\infty} [a_n \sin((2n-1)r\tau/2) + b_n \cos((2n-1)r\tau/2)]. \tag{2}$$

0022-460X/01/430527 + 10 $35.00/0

Substituting equation (2) into equation (1), and equating the like sine and cosine terms produce two sets of algebraic problems of infinite dimension given by

$$\begin{bmatrix} 1-(r/2)^2-\alpha/2 & \alpha/2 & 0 & 0 & \cdots \\ \alpha/2 & 1-(3r/2)^2 & \alpha/2 & 0 & \cdots \\ 0 & \alpha/2 & 1-(5r/2)^2 & \alpha/2 & \cdots \\ 0 & 0 & \alpha/2 & 1-(7r/2)^2 & \cdots \\ \cdots & \cdots & \cdots & \cdots & \cdots \end{bmatrix} \begin{Bmatrix} a_1 \\ a_2 \\ a_3 \\ a_4 \\ \cdots \end{Bmatrix} = \zeta \begin{Bmatrix} rb_1 \\ 3rb_2 \\ 5rb_3 \\ 7rb_4 \\ \cdots \end{Bmatrix} \tag{3}$$

and

$$\begin{bmatrix} 1-(r/2)^2+\alpha/2 & \alpha/2 & 0 & 0 & \cdots \\ \alpha/2 & 1-(3r/2)^2 & \alpha/2 & 0 & \cdots \\ 0 & \alpha/2 & 1-(5r/2)^2 & \alpha/2 & \cdots \\ 0 & 0 & \alpha/2 & 1-(7r/2)^2 & \cdots \\ \cdots & \cdots & \cdots & \cdots & \cdots \end{bmatrix} \begin{Bmatrix} b_1 \\ b_2 \\ b_3 \\ b_4 \\ \cdots \end{Bmatrix} = -\zeta \begin{Bmatrix} ra_1 \\ 3ra_2 \\ 5ra_3 \\ 7ra_4 \\ \cdots \end{Bmatrix} \tag{4}$$

respectively. Note that $f = 0$ here since we are mainly interested in the free dynamic response. Now, let $\mathbf{M}_1$ be the coefficient matrix on the left hand side of equation (3), $\mathbf{M}_2$ be the corresponding matrix in equation (4), $\mathbf{A} = \{a_1, a_2, a_3, \ldots\}^{\mathrm{T}}$, $\mathbf{B} = \{b_1, b_2, b_3, \ldots\}^{\mathrm{T}}$, and

$$\mathbf{R}_1 = \begin{bmatrix} r & 0 & 0 & \cdots \\ 0 & 3r & 0 & \cdots \\ 0 & 0 & 5r & \cdots \\ \cdots & \cdots & \cdots & \cdots \end{bmatrix}. \tag{5}$$

We can then rewrite equations (3) and (4) as $\mathbf{M}_1\mathbf{A} = \zeta\mathbf{R}_1\mathbf{B}$ and $\mathbf{M}_2\mathbf{B} = -\zeta\mathbf{R}_1\mathbf{A}$ respectively. Eliminating $\mathbf{B}$ from these two equations yields $[\mathbf{M}_2(\mathbf{R}_1)^{-1}\mathbf{M}_1 + \zeta^2\mathbf{R}_1]\mathbf{A} = \{0\}$, where $\{0\}$ is the null column vector and $\mathbf{R}_1$ is non-singular. In order to guarantee a non-trivial solution, the following infinite determinant must vanish:

$$|\mathbf{M}_2(\mathbf{R}_1)^{-1}\,\mathbf{M}_1 + \zeta^2\,\mathbf{R}_1| = 0. \tag{6}$$

Equation (6) is in fact a form of Hill's infinite determinant. Note that the form shown above is slightly different from the classical infinite determinant for the undamped Mathieu equation described in most advanced dynamics text. This is due to the presence of the first derivative expression related to the damping term in equation (1), which couples the coefficients of the sine and cosine terms. The solutions to α and r that satisfy equation (6) represent the transition curves separating stability and instability in the parameter plane. The points on these transition curves correspond to the periodic motions with periods equal to $4\pi/r$.

Similarly, we can derive the transition curves corresponding to the periodic motions with periods equal to $2\pi/r$ by assuming the Fourier series solution

$$y(\tau) = b_0 + \sum_{n=1}^{\infty} [a_n \sin(nr\tau) + b_n \cos(nr\tau)]. \tag{7}$$

The resulting pair of algebraic problems for the sine and cosine terms is

$$\begin{bmatrix} 1-r^2 & \alpha/2 & 0 & 0 & \cdots \\ \alpha/2 & 1-(2r)^2 & \alpha/2 & 0 & \cdots \\ 0 & \alpha/2 & 1-(3r)^2 & \alpha/2 & \cdots \\ 0 & 0 & \alpha/2 & 1-(4r)^2 & \cdots \\ \cdots & \cdots & \cdots & \cdots & \cdots \end{bmatrix} \begin{Bmatrix} a_1 \\ a_2 \\ a_3 \\ a_4 \\ \cdots \end{Bmatrix} = 2\zeta \begin{Bmatrix} b_1 \\ 2rb_2 \\ 3rb_3 \\ 4rb_4 \\ \cdots \end{Bmatrix} \tag{8}$$

and

$$\begin{bmatrix} 1-r^2-\alpha^2/2 & \alpha/2 & 0 & 0 & \cdots \\ \alpha/2 & 1-(2r)^2 & \alpha/2 & 0 & \cdots \\ 0 & \alpha/2 & 1-(3r)^2 & \alpha/2 & \cdots \\ 0 & 0 & \alpha/2 & 1-(4r)^2 & \cdots \\ \cdots & \cdots & \cdots & \cdots & \cdots \end{bmatrix} \begin{Bmatrix} b_1 \\ b_2 \\ b_3 \\ b_4 \\ \cdots \end{Bmatrix} = -2\zeta \begin{Bmatrix} ra_1 \\ 2ra_2 \\ 3ra_3 \\ 4ra_4 \\ \cdots \end{Bmatrix}. \tag{9}$$

The static term in equation (7) gives rise to $b_0 = (-\alpha b_1/2)$, which is also used to derive part of the above algebraic equations. By defining $\mathbf{N}_1$ and $\mathbf{N}_2$ to be the coefficient matrices on the left-hand side of equations (8) and (9), respectively, and

$$\mathbf{R}_2 = \begin{bmatrix} r & 0 & 0 & \cdots \\ 0 & 2r & 0 & \cdots \\ 0 & 0 & 3r & \cdots \\ \cdots & \cdots & \cdots & \cdots \end{bmatrix}, \tag{10}$$

the above algebraic problems can also be manipulated like equations (3) and (4) to yield a second Hill's infinite determinant expressed as

$$|\mathbf{N}_2(\mathbf{R}_2)^{-1}\,\mathbf{N}_1 + 4\zeta^2\mathbf{R}_2| = 0. \tag{11}$$

The solutions of α and r that satisfy equation (11) are the transition curves corresponding to the periodic motions with periods equal to $2\pi/r$. Since the determinants in equations (6) and (11) are infinite, it is necessary to limit the number of terms in the Fourier series solutions to ease computational efforts. This will lead to finite size determinants. Based on our analysis, the 9×9 determinants are sufficient to give relatively accurate estimations. The predicted stability boundaries are illustrated in Figure 1. Note that the unstable regions are encompassed by boundary curves corresponding to periodic motions with the same periodicity, while the stable areas are bounded by periodic motions of different periods. Comparison of this new parameter plane to the one published in references [1, 2] shows a number of additional unstable regions at lower values of r, which were not predicted earlier. For the case of $\zeta = 0$, these stability boundaries converge to points on the r-axis corresponding to the vanishing diagonal elements in equations (3), (4), (8) and (9). This is because each diagonal term will produce a zero determinant for $\alpha = 0$ at the convergence points of the transition curves. For periodicity of $4\pi/r$, we obtain $r = 2, 2/3, 2/5, 2/7$, etc., and for periods equal to $2\pi/r$, we get $r = 1, 1/2, 1/3, 1/4$, etc. Note that references [1, 2] only

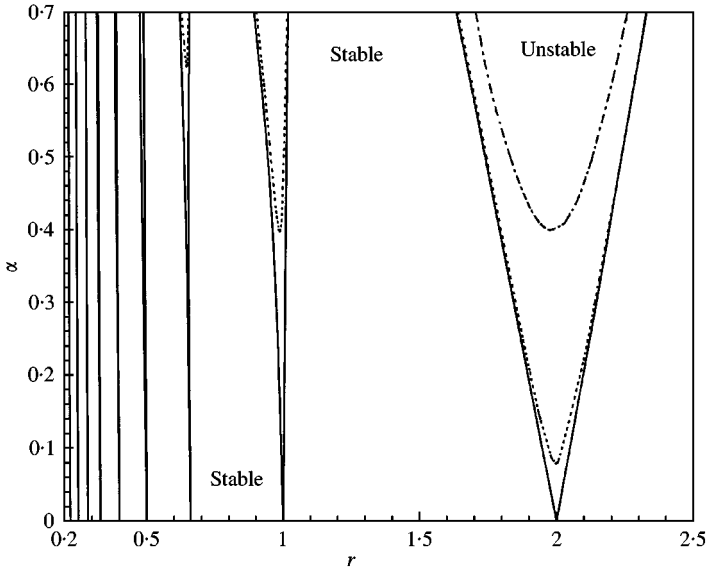

Figure 1. Parameter plane (α, r) of the stable and unstable regions separated by the transition curves corresponding to the periodic motions of the pantograph–catenary system. Note that the transition curves between $r = 0$ and $r = 0{\cdot}2$ are not shown: ——, $\zeta = 0$; ·····, $\zeta = 0{\cdot}02$; – · – · –, $\zeta = 0.1$.

presented the case of $r = 2, 1, 2/3$ even though there is theoretically an infinite number of them between $r = 2$ and 0. These additional points of instability actually explain why the normalized contact force response in Figure 6 of reference [1] peaks in the vicinity of r equals to $1/3$ and $1/2$ in addition to near r equal to 1. The new set of calculations is also confirmed by a series of numerical simulation results applying the 4/5th order Runge–Kutta method. Figures 2 and 3 present the free dynamic responses from the initial condition of $y(0) = 1$ and $(\mathrm{d}y/\mathrm{d}\tau)\,(0) = 0$ for constant $\alpha = 0{\cdot}60$ and $r = 0{\cdot}93$ respectively. In Figure 2, the non-dimensional frequency r is varied, while in Figure 3, different values of stiffness variation coefficient α are evaluated. In all cases shown, the points that fall within the instability areas lead to unbounded motions over time as illustrated in Figures 2(a–f) and 3(b, d), while those that are on the transition curves or outside the instability regions depict stable motions as shown in Figures 3(a, c). From these time domain simulation results, the unbounded growth in dynamic motions occurring at the additional instability points as shown in Figure 2(a–c), which was not mentioned in references [1, 2], supports the validity of our computations.

In addition, the new calculation results for the damped cases ($\zeta \neq 0$) are more conservative than the predictions made by the authors of references [1, 2]. For instance, in the case of $r = 2$ and $\zeta = 0{\cdot}02$, the transition curve separating stability from instability reaches as low as approximately $\alpha = 0{\cdot}08$, while references [1, 2] show a minimum value of about $\alpha = 0{\cdot}45$ that is significantly higher. This resulted in narrower unstable regions in the earlier study compared to the current one. We believe the error was made during the application of the Floquet theory in assessing the stability of the system based on the pair of eigenvalues of the monodromy matrix (also known as the characteristic multipliers [4]), which were computed from the simulated free dynamic response under two specified initial conditions as suggested by Nayfeh and Mook [3]. The problem here is that this approach is meant only for the case of the undamped Mathieu equation. The authors of references [1, 2] must have relied on the simulation results of equation (1) instead of transforming the

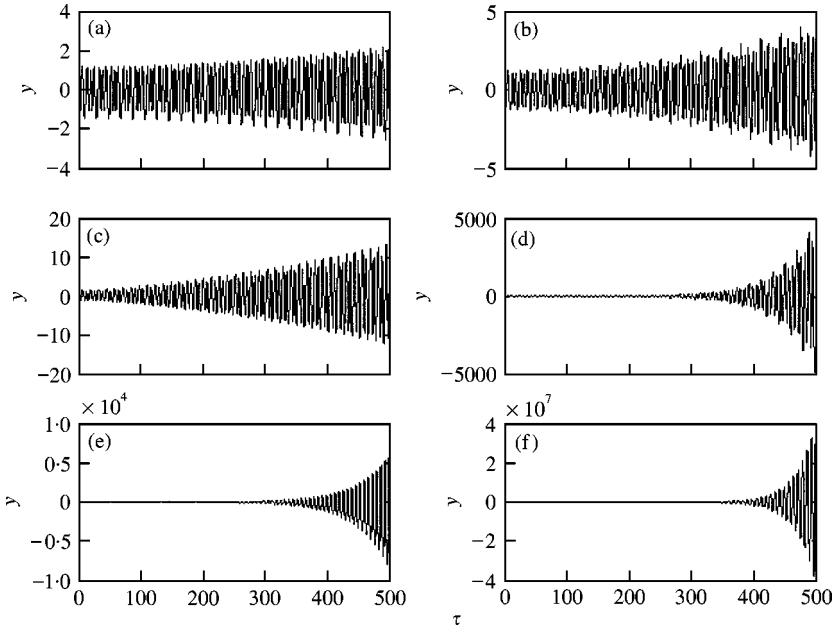

Figure 2. Free dynamic response (unstable) simulation results for $\alpha = 0{\cdot}60$ and $\zeta = 0$ (a) $r = 0{\cdot}325$; (b) $r = 0{\cdot}39$; (c) $r = 0{\cdot}49$; (d) $r = 0{\cdot}65$; (e) $r = 0{\cdot}93$; (f) $r = 1{\cdot}70$.

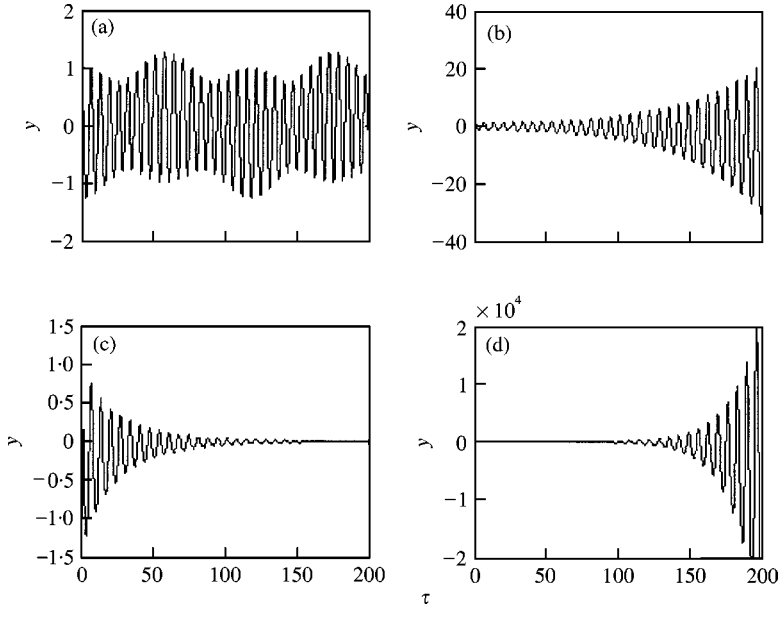

Figure 3. Free dynamic response simulation results for $r = 0{\cdot}93$. (a) $\alpha = 0{\cdot}4$, $\zeta = 0$, periodic; (b) $\alpha = 0{\cdot}6$, $\zeta = 0$, unstable; (c) $\alpha = 0{\cdot}6$, $\zeta = 0{\cdot}05$, stable; (d) $\alpha = 0{\cdot}7$, $\zeta = 0$, unstable.

equation first into the standard Mathieu form that does not explicitly contain any first order derivative expression as shown in the next section. This misapplication actually leads to an erroneous conclusion given in reference [2] when the authors incorrectly identified the dynamic motion for the case of $r = 2$, $\alpha = 0{\cdot}4$ and $\zeta = 0{\cdot}02$ to be bounded. In fact, according

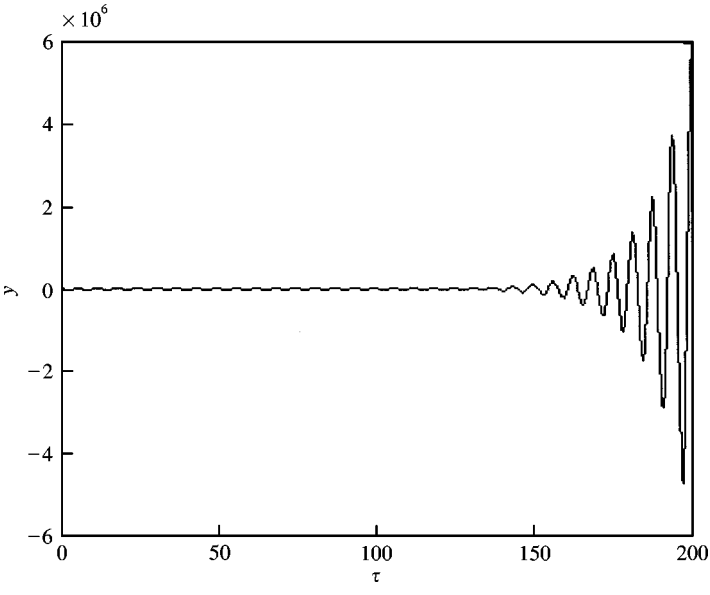

Figure 4. Free dynamic response (unstable) simulation result for the case of $r = 2$, $\alpha = 0{\cdot}4$ and $\zeta = 0{\cdot}02$.

to our stability analysis, it is unstable as shown in the free dynamic response simulation results of Figure 4. To further confirm our suspicion, we retraced the analysis of characteristic multipliers for the case in question by first simulating the free dynamic response using equation (1) and then later using the standard Mathieu equation. Our results show that the predicted absolute value of the trace of the monodromy matrix (which determines the exact form of the characteristic multipliers) is equal to 0·985 in the former case. This value is slightly less than 1, which makes the solution to appear bounded. On the other hand, the latter analysis produces a value of 1·049 that predicts an unbounded solution contrary to the former conclusion. This limited analysis proves our point and also confirms that Hill's method of infinite determinant is more accurate. The misapplication described above, compounded by the use of discrete grid points to calculate the stability boundaries as reported in reference [2], may have also resulted in missing transition curves separating stability from instability at the smaller values of r.

3. STANDARD MATHIEU EQUATION

Suppose we let $r\tau = 2T$, the first and second derivatives in equation (1) become

$$\frac{\mathrm{d}y}{\mathrm{d}\tau} = \frac{r}{2}\frac{\mathrm{d}y}{\mathrm{d}T}, \qquad \frac{\mathrm{d}^2y}{\mathrm{d}\tau^2} = \frac{r^2}{4}\frac{\mathrm{d}^2y}{\mathrm{d}T^2}. \tag{12}$$

Substitution of the above derivatives into equation (1) gives

$$\frac{\mathrm{d}^2y}{\mathrm{d}T^2} + 2\tilde{\zeta}\frac{\mathrm{d}y}{\mathrm{d}T} + (\gamma + 2\varepsilon\cos 2T)\, y = \gamma f, \tag{13}$$

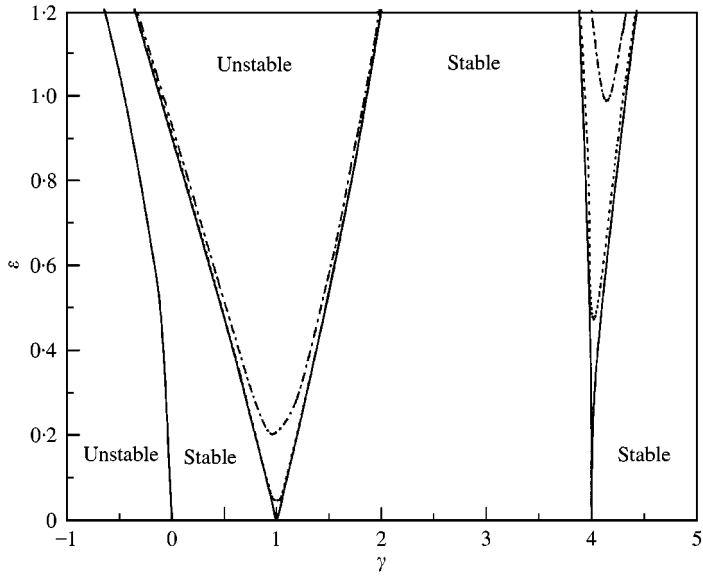

Figure 5. Parameter plane (ε, γ) of the stable and unstable regions separated by the transition curves corresponding to the periodic motions of the pantograph–catenary system: ——, $\tilde{\zeta} = 0$; ·····, $\tilde{\zeta} = 0{\cdot}02$; – · – · – · –, $\tilde{\zeta} = 0{\cdot}1$.

where $\gamma = 4/r^2$, $\varepsilon = 2\alpha/r^2$ and $\tilde{\zeta} = 2\zeta/r$. Applying Hill's method of infinite determinant to the above equation produces another parameter plane (ε, γ) as shown in Figure 5, which is essentially equivalent to the one shown in Figure 1. The stability boundary curves in Figure 5 can be back-transformed into the ones given in Figure 1 by employing $\alpha = 2\varepsilon/\gamma$, $r = 2/\sqrt{\gamma}$ and $\zeta = \tilde{\zeta}r/2$. Note that since α and r are inversely proportional to γ and $\sqrt{\gamma}$, respectively, a horizontal line that goes from $\gamma = 0 \to \infty$ in the parameter plane shown in Figure 5 becomes a curvilinear line that starts from infinity and converges to the origin $(\alpha = 0, r = 0)$ of the parameter plane shown in Figure 1. Therefore, as the horizontal line of $\gamma = 0 \to \infty$ encounters more regions of instability in Figure 5, say for the undamped case, each one of these unstable regions is in fact stacked up increasingly closer together as the corresponding curvilinear line approaches $r = 0$ of the parameter plane in Figure 1. This pattern of additional stability boundary curves is clearly missing from the parameter planes given in references [1, 2] as pointed out earlier. Furthermore, α is directly proportional to the slope ε/γ of a straight line emanating from the origin of Figure 5. Thus, the steeper the line becomes (larger α), the greater the region of instability is encountered, which is exactly as depicted in the parameter plane of Figure 1.

We can further introduce the transformation

$$y = x\mathrm{e}^{-2\zeta T/r}, \tag{14}$$

which converts equation (13) in the standard Mathieu form given by

$$\frac{\mathrm{d}^2x}{\mathrm{d}T^2} + (\delta + 2\varepsilon\cos 2T)\,x = \tilde{f}, \tag{15}$$

where $\delta = 4(1 - \zeta^2)/r^2$ and $\tilde{f} = (4f/r^2)\,\mathrm{e}^{(2\zeta T/r)}$. Recall that equation (15) is applied earlier to demonstrate the calculation of the characteristic multipliers. Since it is well studied, one can

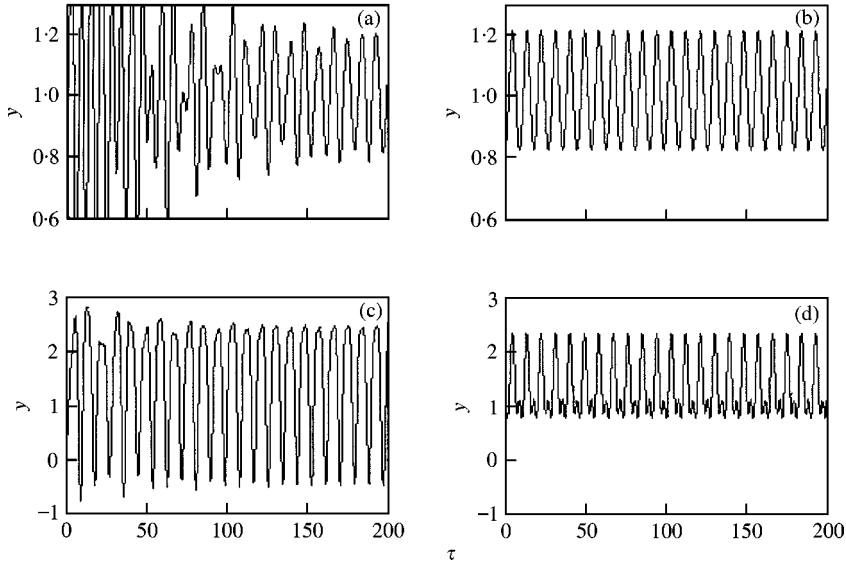

Figure 6. Comparison of the forced response time histories predicted by the proposed analytical solution presented in reference [1] and our direct numerical integration simulation for the case of $r = 0{\cdot}7$, $\zeta = 0{\cdot}02$, $f = 1$, $y(0) = 0$ and $(dy/d\tau)\ (0) = 0$: (a) $\alpha = 0{\cdot}1$, numerical simulation; (b) $\alpha = 0{\cdot}1$, analytical prediction; (c) $\alpha = 0{\cdot}6$, numerical simulation; (d) $\alpha = 0{\cdot}6$, analytical prediction.

simply apply the available published solutions including its parameter plane (generally known as the Strutt diagram [3, 4]) to further approximate the dynamic characteristics of the pantographcatenary system. However, there is a limitation. Because of the use of the transformation defined by equation (14) to eliminate the first order derivative term, the points of instability predicted by the standard Strutt diagram of equation (15) may some time be indeed stable. This is especially true for points near the stability boundaries due to the stabilizing effect of the viscous damping. The effect is actually depicted in equation (14) where the second term given by $e^{-2\zeta T/r}$ may be sufficient, depending on the level of the damping present, to overcome the unbounded response of $x(T)$. Hence, the solution obtained directly from the standard Strutt diagram is slightly conservative.

4. FORCED RESPONSE

Next, the limitations of the steady state forced response formulation given by equation (5) in reference [1] are discussed. Since the straightforward perturbation method is used to formulate the forced response equation, which is based on a series expansion about the linear time-invariant generating solution, the resultant expression should theoretically be valid only for small variation in the stiffness coefficient within the stable region. Therefore, the predictions by this proposed equation are closest to the actual steady state response when α is relatively small. The deviation between the approximate and actual solutions should increase for larger values of α. This trend is actually shown in Figure 6 for the case of $r = 0{\cdot}7$, $\zeta = 0{\cdot}02$ and $f = 1$. By changing α from 0·1 to 0·6, we observe a greater difference between the proposed analytical prediction of reference [1] and our direct numerical integration solutions (with no simplifying assumption). In addition, the proposed approximate forced response solution neglects the transient response due to the initial

conditions, which in some cases do not vanish, but instead lead to a limit cycle behavior. This is especially true at the parameter points on the transition curves separating stability from instability in which periodic motions are predominant.

5. CONCLUDING REMARKS

The stability analysis of the pantograph–catenary system based on Hill's method of infinite determinant clearly reveals additional unstable areas at lower values of r not mentioned in references [1, 2]. The new parameter plane depicting transition curves separating stability from instability is validated using the free dynamic response results. We also pointed out the misapplication of the Floquet theory to the damped Mathieu equation resulting in less conservative solutions and missing instability regions. Furthermore, the analytical solution for the steady state forced response derived from the straightforward perturbation method is shown to be limited to only small values of α. Finally, we think these reported discrepancies do not actually alter the main conclusions of the earlier study [1, 2], but it does provide a more complete characterization of the stability behavior and points out an obvious misapplication of the Floquet theory.

REFERENCES

1. T. X. Wu and M. J. Brennan 1999 *Journal of Sound and Vibration* **219**, 483–502. Dynamic stiffness of a railway overhead wire system and its effect on pantograph–catenary system dynamics.
2. T. X. Wu and M. J. Brennan 1998 *Vehicle System Dynamics* **30**, 443–456. Basic analytical study of pantograph-catenery system dynamics.
3. A. Nayfeh and D. T. Mook 1979 *Nonlinear Oscillations*. New York: John Wiley & Sons.
4. L. Meirovitch 1970 *Methods of Analytical Dynamics*. New York: Mc-Graw Hill.

AUTHORS' REPLY

T. X. Wu and M. J. Brennan

*Institute of Sound and Vibration Research, University of Southampton, Southampton SO*17 1*BJ, England. E-mail: mjb@isvr.soton.ac.uk*

(*Received* 26 *February* 2001)

The authors wish to thank Guan and Lim [1] for their interest in the material presented in references [2, 3]. The comments made by them are correct and thus the reader of references [2, 3] is referred to Figure 1 in reference [1] to replace Figure 5 in reference [2] and Figure 4 in reference [3] as a correction. However, this does not affect the main results and conclusions in references [2, 3], since the damping of a pantograph-catenary system is large enough to maintain the response of the system always within the stable region. This has also been pointed out by Guan and Lim in their concluding remarks [1].